

Polarization Experiments in High Energy  
Pion-Nucleon Elastic Scattering

L. Van Rossum

C.E.N.-Saclay

A. CERN EXPERIMENTS ON POLARIZATION AND SPIN-ROTATION AT  $\mathcal{P}_{\text{LAB}} > 6 \text{ GEV}/c$   
(1967-1971).

A.1. Introduction.

The scattering matrix for pion-nucleon elastic scattering or charge exchange depends on two complex amplitudes, functions of the center of mass energy  $s$  and the four-momentum transfer  $t$ . Different representations may be used for the amplitudes (Pauli-spinor amplitude, invariant amplitude, s- or t-channel helicity amplitudes, etc...). For any representation it is possible to determine the two moduli and the relative phase by an appropriate set of three measurements at given values of  $s$  and  $t$ . In addition, the absolute phase can be determined at  $t = 0$  from the ratio of the real to the imaginary part of the forward scattering amplitude, given by experiment and by dispersion relations. At  $t \neq 0$ , the three independent observables to be measured are the unpolarized differential cross-section  $I(s,t) = \frac{d\sigma}{dt}$ , and two polarization parameters.

The unpolarized differential cross-section is proportional to the probability for scattering averaged over all possible spin states of the proton before and after scattering. The target is unpolarized and the detectors are not sensitive to the polarization of the recoil protons.

In the polarization experiments the initial state is a polarized one (polarized target), and (or) the polarization of the recoil protons must be measured. Both the target protons and the recoil protons at given angles  $\theta$  and  $\varphi$  are statistical mixtures of pure spin states. The initial and the final polarizations are described by spin density matrices which are related to each other by the scattering matrix. The physical quantities directly accessible to experiment are the transverse and longitudinal components of the initial and the final polarization. The so called "polarization parameters" are three scalars, functions of  $s$  and  $t$ , relating the three components of the final polarization  $\vec{P}_f$  to the three components of the initial polarization  $\vec{P}_i$ . These functions describe the dynamics of spin effects and may be considered as the spin dependent "observables". Only two of them are independent observables, the sum of the squares of the three parameters being equal to 1.

... / ...

The definition of the polarization parameters depends on the system of reference used to decompose the polarization vectors. The convention used most frequently in the recent literature on pion-nucleon scattering is to decompose the initial polarization  $\vec{P}_i$  into

$$\vec{P}_i = |\vec{P}_i| \cdot \left\{ \begin{array}{l} \hat{k}_i \\ \hat{n} \\ \hat{k}_i \times \hat{n} \end{array} \right\}$$

and to decompose the final polarization  $\vec{P}_f$  into

$$\vec{P}_f = |\vec{P}_f| \cdot \left\{ \begin{array}{l} \hat{k}_p \\ \hat{n} \\ \hat{k}_p \times \hat{n} \end{array} \right\}$$

where  $\hat{k}_i$  and  $\hat{k}_f$  are the unit momentum vectors of the incident and the scattered pion respectively, and where  $\hat{k}_p$  is the unit momentum vector of the recoil proton in the laboratory frame. The normal to the scattering plane  $\hat{n}$  is defined as

$$\hat{n} = \frac{\hat{k}_i \times \hat{k}_f}{|\hat{k}_i \times \hat{k}_f|}$$

(The directions of  $\hat{k}_i$  and  $\hat{n}$  do not depend on whether  $\vec{k}_i$  and  $\vec{k}_f$  are defined in the laboratory frame or in the center of mass frame).

This convention about the systems of reference introduces the transverse and longitudinal polarization components in the laboratory frame. It is analog to Wolfensteins description of polarization and spin rotation in proton carbon elastic scattering.

The three polarization parameters P, R and A for pion-nucleon scattering, are defined by the relations between the initial and the final polarization components, with this particular choice of the systems of reference, (Table 1).

The P parameter is given by the polarization  $\vec{P}_f$  of the recoil protons when the target is unpolarized ( $\vec{P}_i = 0$ ). In this case parity conservation requires that  $\vec{P}_f$  has the direction  $\pm \hat{n}$ . The sign convention used in pion nucleon scattering is that P is positive when the recoil protons are polarized along  $+\hat{n}$ . The magnitude of  $\vec{P}_f$  is equal to the absolute value of P. Application of the spin density matrix formalism shows that P can also be determined by measuring the left-right asymmetry for scattering on a polarized proton target with a polarization  $\vec{P}_i$  normal to the scattering plane.

... / ...

In order to determine the spin rotation parameters  $R$  and  $A$ , or a linear combination, the target must be polarized along a direction contained within the scattering plane and either the longitudinal or the transverse component in the scattering plane must be measured in the final state.

The moduli of the two scattering amplitudes and their relative phase are given by the unpolarized differential cross-section  $I(s,t)$  and two of the three polarization parameters  $P(s,t)$ ,  $R(s,t)$  and  $A(s,t)$ . Table 2 shows the expressions relating observables and scattering amplitudes in the case of  $s$ -channel helicity amplitudes.

Complete experimental knowledge of pion-nucleon elastic scattering and charge exchange therefore requires three independent measurements at all values of  $s$  and  $t$ , for each of the two isospin states. Once this situation is realized, the confrontation of theories or models with experiment will no longer take the form of predictions for particular observables, or model fits to individual data points. It will consist in comparing the experimental amplitudes with those proposed by theory.

At present, complete sets of experiments exist only at 6 GeV/c incident momentum, for  $-t$  ranging from 0.2 to 0.5 (GeV/c)<sup>2</sup>.

The polarization experiments in pion nucleon scattering at  $P_{\text{LAB}} > 6$  GeV/c are those carried out at CERN from 1967 to 1971, and those now in progress at the Serpukhov accelerator, (Table 3). The four-momentum transfer ranges from about  $-t = 0.1$  (GeV/c)<sup>2</sup> up to  $-t = 2.0$  (GeV/c)<sup>2</sup> for some of the experiments.

The data used in the amplitude analysis come from the CERN-ORSAY-PISA experiment for  $P$  in elastic scattering [1-3], from the DESY-SACLAY experiment for  $P$  in pion-nucleon charge exchange [4] and from the SACLAY experiment for  $R$  and  $A$  [5].

#### A.2. $P$ in $\pi^+p$ elastic scattering (CERN-ORSAY-PISA) [1-3]

The principle of  $P$  measurements with a polarized target is the following :

A measurement of the left-right asymmetry for scattering on a target with fixed polarization, normal to the scattering plane, would require exactly equal (or exactly known) detection efficiencies for scattering to the left and to the right. In the case of rapidly varying differential cross section, this method would also be very sensitive to small errors in determining the effective beam direction with respect to which the angles are measured. These

difficulties can be avoided by replacing the measurement of

$$I \begin{matrix} \text{UP} \\ \text{RIGHT} \end{matrix} \text{ by } I \begin{matrix} \text{DOWN} \\ \text{LEFT} \end{matrix} \left( \text{or } I \begin{matrix} \text{UP} \\ \text{LEFT} \end{matrix} \text{ by } I \begin{matrix} \text{DOWN} \\ \text{RIGHT} \end{matrix} \right), \text{ "UP" and "DOWN" referring}$$

to the sign of the target polarization.

In fact

$$P = \frac{1}{|\vec{P}_i|} \frac{I_{\text{LEFT}}^{\text{UP}} - I_{\text{RIGHT}}^{\text{UP}}}{I_{\text{LEFT}}^{\text{UP}} + I_{\text{RIGHT}}^{\text{UP}}} = \frac{1}{|\vec{P}_i|} \frac{I_{\text{LEFT}}^{\text{UP}} - I_{\text{LEFT}}^{\text{DOWN}}}{I_{\text{LEFT}}^{\text{UP}} + I_{\text{LEFT}}^{\text{DOWN}}}$$

because the equivalent measurements differ only by a rotation of  $180^\circ$  around the beam axis.

The P parameter is, therefore, proportional to the relative change in counting rate corresponding to reversal of target polarization.

The counting rates to be considered are those for elastic scattering on free (polarized) protons in the target. Counts from all other types of interaction must be suppressed or subtracted. The most powerful method for reducing background counts consists in checking the coplanarity of the incident and the outgoing trajectories, and the correlation of the scattering angles for the outgoing particles. Elastic scatterings on free protons appear as peaks in appropriate distributions, whereas background events show a smooth behaviour. The amount of background under the "hydrogen peak" is typically of the order of 10 percent at small momentum transfer, and increases to about 50% or more at large  $t$ .

The results (Fig. 1 a, b) show that at all energies, the value of P rises to a maximum at about  $-t = 0.3 \text{ (GeV/c)}^2$  followed by a minimum at  $-t \approx 0.6 \text{ (GeV/c)}^2$ . P in  $\pi^+p$  and  $\pi^-p$  elastic scattering exhibits approximate mirror symmetry :

$$P \begin{matrix} (t) \\ \pi^+p \end{matrix} \approx - P \begin{matrix} (t) \\ \pi^-p \end{matrix}$$

the polarization for  $\pi^+p$  scattering being positive.

The maximum of polarization at  $-t \approx 0.3 \text{ (GeV/c)}^2$  decreases with increasing  $s$ .

### A.3. P in $\pi^-p$ charge exchange (DESY-SACLAY) [4]

The principle of measurement is the same as for elastic scattering. The direction of the  $\pi^0$  is determined from the showers produced by the pair of photons. The direction of the neutron can be measured by neutron detectors and its momentum can be determined by time of flight. However, the experiments at 5 GeV/c and at 8 GeV/c have not used any detection of the neutron, because the low efficiency of these detectors would have led to prohibitively low counting rates. The main selection criterium was the absence of charged particles or additional  $\gamma$ -rays in the final state. Without kinematic selection of charge exchange on free protons, the background to be subtracted represents about 3/4 of the total counting rate, and because of the dip structure of the differential cross-section, this ratio is not a smooth function of  $t$ .

The results (Fig. 2) show a positive polarization which rises to a maximum at  $-t \simeq 0.5$  GeV/c. In this experiment the maximum is of the order of  $P \simeq +0.5$  or more, at 5 GeV/c incident momentum.

### A.4. R and A in $\pi^+p$ elastic scattering (SACLAY) [5]

Measurements of spin rotation parameters require to scatter pions on a proton target that is polarized along a direction in the scattering plane, and to analyze the polarization of the recoil protons in a polarimeter.

The accessible interval of four-momentum transfer is fixed by instrumental limitations. It lies between  $t = -0.19$  (GeV/c)<sup>2</sup> and  $t = -0.51$  (GeV/c)<sup>2</sup>. Measurements at higher values of  $|t|$  would imply prohibitively low counting rates and, because of the high energy of the recoil protons, it would be more difficult to analyse their polarization. Measurements at  $|t| < 0.19$  (GeV/c)<sup>2</sup> are made difficult by the large energy loss and multiple scattering of the recoil protons in the target. Also, the analysis of protons with less than 100 MeV kinetic energy would require a different technique.

The target magnet must present a minimum of obstructions for particles scattered in a plane that contains the direction of the magnetic field. The most adequate solution was to build a superconducting air core magnet with high current density. The recoil protons, emitted at a mean angle of 72° with respect to the beam, enter the polarimeter about one meter from the target.

This detector is made of Carbon plates alternated with wire spark chambers with core read-out. Seven scintillation counter hodoscopes associated with a fast logic allow the spark chambers of the polarimeter to be triggered mainly on elastic scatterings off the free protons in the target.

The experiment was carried out at CERN in 1968 and 1969. The main features of the results are the following (Fig. 3 a-c): A is always close to +1, while R is small and negative, with a possible exception for  $R(\pi^+p)$  at 6 GeV/c, at low four-momentum transfer. Both parameters show only weak dependence on  $t$  within the interval covered by the experiment.  $R(\pi^-p)$  seems to be smaller than  $R(\pi^+p)$  at 6 GeV/c.  $R(\pi^-p)$  and  $A(\pi^-p)$  at 16 GeV/c are not far from  $R = -\cos \Theta_p$  and  $A = +\sin \Theta_p$ , where  $\Theta_p$  is the laboratory angle of the recoil proton. These would be the values for R and A, at all energies, if direct channel helicity flip is absent.

#### B. AMPLITUDE ANALYSIS OF $\pi$ N SCATTERING AT 6 AND 16 GEV/C.

The results of a combined analysis of the measurements of P, R and A at CERN energies [1-5] together with the data for the differential cross-sections [6] have been used for an amplitude analysis of the pion-nucleon scattering at 6 and 16 GeV/c [7]. In terms of the s-channel helicity amplitudes we can write :

$$\frac{\sqrt{\pi}}{q} f_{\substack{(s) \\ ++ \\ (+-)}} \left\{ \begin{array}{l} \pi^+p \\ \pi^-p \end{array} \right\} = F_{\substack{\circ \\ ++ \\ (+-)}} \left\{ \begin{array}{l} - \\ + \end{array} \right\} F_{\substack{1 \\ ++ \\ (+-)}}$$

for elastic scattering, and

$$\frac{\sqrt{\pi}}{q} f_{\substack{(s) \\ ++ \\ (+-)}} \left\{ \text{CEX} \right\} = -\sqrt{2} F_{\substack{1 \\ ++ \\ (+-)}}$$

for charge exchange scattering.  $F^0$  and  $F^1$  are the amplitudes for the isospin  $T = 0$  and  $T = 1$  states in the crossed channel, and  $q$  is the center of mass momentum. The amplitudes  $f^{(s)}$  are related to the observables by the expressions given in Table 2.

At 6 GeV/c incident momentum the existing data amount to 8 independent observables for 7 parameters. The absolute value of A is obtained from

$$A = \pm \sqrt{1 - P^2 - R^2}. \quad \text{The sign of A is given by the direct measurement}$$

of this observable in  $\pi^-p$  elastic scattering, yielding  $A \approx 0$ .

This means that, as expected,  $f_{++}^{(s)}(\pi^-p) \approx f_{+-}^{(s)}(\pi^-p)$  in the  $t$ -region under consideration. The same must be true for  $\pi^+p$  scattering, since elastic scattering is dominated by  $F^0$ . The resulting magnitudes of the pion-nucleon amplitudes  $F_{++}^0$ ,  $F_{+-}^0$ ,  $F_{++}^1$  and  $F_{+-}^1$  are shown on Fig. 4. Since  $R$  measurements exist only up to  $t = -0.5$  (GeV/c)<sup>2</sup>, the results at larger momentum-transfer depend on the functions used to fit the data for this observable. Since only relative phases of the amplitudes can be obtained from these measurements, fig. 5 represents the complex ratios. The relative phases with respect to the dominating amplitude  $F_{++}^0$  are plotted assuming this amplitude to be purely imaginary. Since this is approximately true at small  $t$ , the graphs represent approximately the absolute phases of  $F_{++}^1$  and  $F_{+-}^1$ . The relative phase of  $F_{+-}^0$  with respect to  $F_{++}^0$  is always close to 180°.

The predictions for  $R$  and  $A$  in pion-nucleon charge exchange do not depend on the absolute phases (fig. 6). First order zeros of  $A$  are expected when the difference  $|F_{++}^1| - |F_{+-}^1|$  changes sign. First order zeros of  $R$  are expected in the vicinity of the minima of  $|F_{++}^1|$  and  $|F_{+-}^1|$  where the phase difference of these two amplitudes goes through 90°.

At 16 GeV/c we do not know the polarization in charge exchange, and  $R$  has been measured only in  $\pi^-p$  elastic scattering. The six existing observables are not sufficient to determine the amplitudes, especially for isospin  $T = 1$  exchange. Only the  $F^0$  amplitudes are given with a reasonable precision. The  $t$ -dependence of  $|F_{++}^0|$  and  $|F_{+-}^0|$  is very similar to the one at 6 GeV/c, the relative phase of  $F_{+-}^0$  with respect to  $F_{++}^0$  is very close to 180°, similarly to the situation at 6 GeV/c.

How do the experimental amplitudes at 6 GeV/c compare with predictions of specific theories or models? The answer is that all main features of the experimental data are known since the Lund Conference in 1969, and that, therefore, the experimental amplitudes are compatible with all recent models. As an example we may consider Regge pole theory. This theory makes very specific predictions about the phases and a first step would be to estimate the phase  $\xi_{++}^0(t)$  of  $F_{++}^0$  which was used as reference. At  $t = 0$ ,  $\xi_{++}^0$  is given directly by the ratios  $r^+$  and  $r^-$  of the real to the imaginary parts of the  $\pi^\pm p$  forward scattering amplitudes. These ratios are known from experiment and from dispersion relations. At 6 GeV/c  $\xi_{++}^0(t=0) \approx 100^\circ$ , since  $\frac{r^+ + r^-}{2} \approx \text{ctg } \xi_{++}^0 \approx -0.2$ . The  $t$ -dependence of  $\xi_{++}^0$  is unknown unless we use a model.



If we want to compare the experimental amplitudes with those proposed by Regge pole theory, it is reasonable to use the Regge phases for  $\xi_{++}^{\circ}(t)$ . The phase at  $t = 0$  determines the relative strength of Pomeron to  $f_0$  coupling. Assuming this ratio to be true also for  $t \neq 0$ , and using the standard slopes of the two trajectories, we find that  $\xi_{++}^{\circ}(t)$  increases slowly with  $|t|$  and reaches the value of  $\xi_{++}^{\circ} \simeq 130^{\circ}$  at  $t = -1.0$   $(\text{GeV}/c)^2$ .

With these Regge assumptions about the phase of  $F_{++}^{\circ}$ , it is possible to calculate the absolute phases and to present the results in form of diagrams showing the  $t$ -dependence of the imaginary and the real parts of each of the four amplitudes. The results of an approximate calculation are shown on fig. 7 and 8 for the amplitudes with isospin  $T = 1$  exchange.

The simultaneous vanishing of  $\text{Re } F_{+-}^1$  and  $\text{Im } F_{+-}^1$  at  $t \simeq -0.65$   $(\text{GeV}/c)^2$  which is an intrinsic result independent of the absolute phases, is in agreement with the description of  $T = 1$  exchange by exchange of the  $\rho$  trajectory, and with the interpretation of the polarization in elastic scattering by Pomeron- $\rho$  interference. Regge theory alone does not necessarily require this amplitude to vanish when  $\alpha_{\rho} = 0$  at  $t \simeq -0.65$ . But duality imposes a zero of the corresponding amplitude. The experimental symptoms are the dip in  $\frac{d\sigma}{dt}$  for charge exchange, and the vanishing of  $P$  in elastic scattering.

The marked difference of the  $t$ -dependence for  $\text{Im } F_{+-}^1$  and  $\text{Im } F_{++}^1$  is explained by Regge cuts which, at small momentum transfer have a strong effect on  $\text{Im } F_{++}^1$ , but affect only weakly  $\text{Im } F_{+-}^1$ . In diffraction models based on the Harari-Freund conjecture, this difference is a necessary consequence of the assumption that  $T = 1$  exchange is a peripheral interaction. The exact  $t$ -dependence of  $\text{Im } F_{++}^1$  and  $\text{Im } F_{+-}^1$  depends on our assumptions about the absolute phase of  $F_{++}^{\circ}$ .<sup>\*</sup> The experimental symptom corresponding to the zero of  $\text{Im } F_{++}^1$  is the cross-over of the differential cross-sections for  $\pi^{\pm}p$  elastic scattering at  $t = -0.1$  or  $-0.2$   $(\text{GeV}/c)^2$ .

The amplitudes for  $T = 1$  exchange depend particularly on the data for polarization in charge exchange. The analysis<sup>[7]</sup> uses the CERN data at 5 and 8  $\text{GeV}/c$ . An independent analysis<sup>[8]</sup> has been carried out using the ARGONNE data at 5  $\text{GeV}/c$ <sup>[9]</sup>. Around  $t = -0.5$   $(\text{GeV}/c)^2$  there exists a significant discrepancy between the two sets of data at 5  $\text{GeV}/c$ , and the analysis based on the ARGONNE data shows some quantitative difference. It would be very useful to repeat polarization measurements in pion-nucleon charge exchange at 5 or 6  $\text{GeV}/c$ .

... / ...

---

\* In particular, the sign of  $\text{Im } F_{+-}^1$  at  $|t| > 0.5$   $(\text{GeV}/c)^2$  is still undetermined.

For isospin  $T = 0$  exchange the amplitude  $F_{+-}^{\circ}$  is smaller in magnitude than the non-flip amplitude by about one order of magnitude. Its relative phase with respect to  $F_{++}^{\circ}$  is between  $160^{\circ}$  and  $180^{\circ}$ , both at 6 and at 16 GeV/c. The interference of the two isospin  $T = 0$  amplitudes, therefore, contributes only weakly to the polarization in elastic scattering. The ratio  $|F_{+-}^{\circ}| / (|F_{++}^{\circ}| \sqrt{s_0/-t})$  which may be considered as a test of s-channel helicity conservation for  $T = 0$  exchange, is significantly different from zero. In the region from  $t = -0.2$  to  $-0.5$  (GeV/c)<sup>2</sup> this ratio is  $0.17 \pm 0.02$  at 6 GeV/c and  $0.14 \pm 0.03$  at 16 GeV/c.<sup>-</sup> The preceding conclusions concerning  $F_{+-}^{\circ}$  are intrinsic results of the amplitude analysis in the sense that they do not depend on the absolute phases. With the same assumptions made earlier about  $\xi_{++}^{\circ}(t)$ , the amplitude  $F_{+-}^{\circ}$  is mainly negative imaginary, with a slowly increasing positive real part. This rises the question if the helicity flip in  $T = 0$  exchange is characteristic of the Pomeron, or if it can be attributed entirely to  $f_0$  exchange. The present values of the phase, and the weak s-dependence of the ratio of flip to non-flip amplitudes does not favor the latter assumption.

### C. SERPUKHOV POLARIZATION EXPERIMENT (1971-1974) [10,11]

In the Serpukhov experiment (Fig. 9a) the target is polarized in the horizontal plane, perpendicular to the beam. The recoil protons from scattering in the horizontal plane are analyzed in a polarimeter, yielding R, (Fig. 9b). At the same time the asymmetry for scattering in the vertical plane is measured and yields P, (Fig. 9c). Measurements of P and R in a 40 GeV/c negative particle beam have been completed recently. For  $\pi^-p$  elastic scattering P has been measured at four-momentum transfers from  $t = -0.08$  to  $-1.5$  (GeV/c)<sup>2</sup>, and R from  $t = -0.19$  to  $-0.55$  (GeV/c)<sup>2</sup>. For  $K^-p$  elastic scattering P has been measured from  $t = -0.08$  to  $-0.8$  (GeV/c)<sup>2</sup>, and for R an average value for the interval from  $-0.2$  to  $-0.5$  (GeV/c)<sup>2</sup> is obtained.

For P in  $\pi^-p$  elastic scattering (Fig. 10), the polarization is  $P \approx -0.05$  at small momentum transfer, in the region from  $t = -0.1$  to  $-0.3$  (GeV/c)<sup>2</sup>. This value may be compared to  $P \approx -0.09$  at 14 GeV/c. The s-dependence of P at small t, above 6 GeV/c incident momentum, is well fitted by  $P \propto s^{-a}$  with  $a = 0.52 \pm 0.05$  (Fig. 11). At larger t values, between  $-1.0$  and  $-1.5$  (GeV/c)<sup>2</sup>, the polarization P is small and certainly less than 10 per cent. Comparison with the CERN data at 6, 10 and 14 GeV/c [1-3] shows that

---

<sup>-</sup> with  $s_0 = 1 \text{ GeV}^2$

the polarization at large momentum transfer decreases rapidly with energy, with a slope of  $s^{-1}$  or more (Fig. 12). The polarization data at both small and large momentum transfer are compatible with the interpretation of the polarization in  $\pi^- p$  scattering by  $\rho$  and Pomeron interference. Predictions by different Regge pole models and quasipotential models [12-15] are shown on figure 10.

For  $P$  in  $K^- p$  elastic scattering at 40 GeV/c (Fig. 13) the polarization is very small up to  $t = -0.2$  (GeV/c)<sup>2</sup>. The sign of  $P$  in this interval is not defined within the present errors. From  $t = -0.2$  to  $-0.8$  (GeV/c)<sup>2</sup>  $P$  is positive and increases smoothly. At  $t = -0.6$  (GeV/c)<sup>2</sup> it reaches a value of  $P = +(0.04 \pm 0.02)$ . Comparison with the data at 6, 10 and 14 GeV/c shows that  $K^- p$  polarization at this momentum transfer decreases with energy as  $s^{-(1.5 \pm 0.5)}$  (Fig. 14). The data are not inconsistent with the description of  $K^- p$  scattering by Regge pole models with exchange degeneracy.

The spin-rotation parameter  $R$  in  $\pi^- p$  elastic scattering at 40 GeV/c (Fig. 15) is negative, and similar in magnitude and in  $t$ -dependence to the values measured previously at 6 and 16 GeV/c. The data are close to the values expected if the  $s$ -channel helicity-flip amplitude or the spin-flip amplitude is identical to zero. Predictions of a five pole Regge model [13] and of a model with Regge-Pomeron-Regge cuts [14] are shown on figure 4.

For  $R$  in  $K^- p$  elastic scattering at 40 GeV/c, the experiment yields only a mean value, averaged over the interval from  $t = -0.2$  to  $-0.5$  (GeV/c)<sup>2</sup>. This value,  $R_{avr} = -(0.09 \pm 0.23)$ , is consistent, within large statistical errors, with  $R$  in  $\pi^- p$  scattering at the same energy.  $R_{K^- p}(t) \approx R_{\pi^- p}(t)$  is expected if the amplitudes for isospin  $I = 0$  exchange are the dominating ones in both of the reactions at this energy.

The data for  $P$  and for  $R$  in  $\pi^- p$  and  $K^- p$  scattering at small momentum transfer,  $|t| < -0.6$  (GeV/c)<sup>2</sup>, will probably be fitted without difficulty by an extrapolation to 40 GeV/c of any of the existing models.

The small value found for  $P$  in  $\pi^- p$  scattering at larger momentum transfer, between  $t = -1.0$  and  $-1.5$  (GeV/c)<sup>2</sup>, corresponds to an effective  $\rho$ -trajectory showing no evidence for strong cut effects.

With respect to an eventual determination of the pion-nucleon scattering amplitudes at 40 GeV/c from a sufficient set of experiments, only 3 of the required 7 measurements have been carried out so far.

At last comment concerns the relations between the polarization parameters in pion-nucleon and in nucleon-nucleon scattering at high energies. If, at small  $t$  and sufficiently large  $s$  meson-nucleon and nucleon-nucleon elastic scattering is dominated by a single trajectory of natural parity, factorization reduces the nucleon-nucleon amplitudes from five to three, two of which (single flip and double flip) are related to each other. The polarization  $P$  would be zero, but the spin rotation parameters do not vanish.  $R_{\pi p}(s,t)$  and  $R_{pp}(s,t)$  would be equal to each other, irrespectively of the ratio of helicity flip to non-flip amplitudes.

Data for  $R_{pp}$  (Fig. 16) have been presented at the Batavia Conference at 6 and at 16 GeV/c<sup>[16]</sup>. One observes that  $R_{pp}$  at 16 GeV/c is very close to  $R_{\pi-p}$  at the same incident momentum. This is the situation one expects if factorization holds, knowing that the  $T = 0$  amplitude dominates. At the same time one observes that both  $R_{pp}$  and  $R_{\pi-p}$  exhibit a  $t$ -dependence close to  $R = -\cos \theta_p$  which is the relation expected if  $s$ -channel helicity is conserved.

A complete determination of the amplitudes for  $pp$  scattering is more difficult to perform than for  $\pi p$  scattering. If, however, factorization is assumed for the leading Regge poles  $P$  and  $f_0$ , the relations between the  $\pi p$  and  $pp$  amplitudes for exchange of these trajectories reduce the number of free parameters.

The main motivation for continuing the Serpukhov experiment with a positive particle beam are the measurements of  $P$  and  $R$  in proton-proton elastic scattering at 40 or 50 GeV/c.

REFERENCES.

- [1] M.Borghini et al., Phys.Lett. 31B (1970) 405.
- [2] M.Borghini et al., Phys.Lett. 36B (1971) 493.
- [3] M.Borghini et al., CERN Preprint (Jan.15, 1972) to be published in Phys.Lett.
- [4] P.Bonamy et al., Nuclear Physics, B52 (1973) 392.
- [5] A.de Lesquen et al., Phys.Lett. 40B (1972) 277.
- [6] G.C.Fox and C.Quigg, Report UCLR 20001.
- [7] G.Cozzika et al., Phys.Lett. 40B (1972) 281.
- [8] P.Johnson et al., Phys.Rev.Lett., 30 (1973) 242.
- [9] D.Hill et al., Phys.Rev.Lett., 30 (1973) 239.
- [10] C.Bruneton et al., Phys.Lett. 44B (1973) 471.
- [11] Measurements of the polarization parameters P and R in  $\pi^-p$  and  $K^-p$  elastic scattering at 40 GeV/c. Contributed paper n°431, 2<sup>nd</sup> AIX-en-PROVENCE Intern. Conf. on Elementary Particles, September 1973.
- [12] G.Arkelyan et al., Quasieikonal Model for  $\pi N$  scattering. Paper submitted to the 16<sup>th</sup> Intern.Conf. on High Energy Physics, BATAVIA 1972.
- [13] V.Barger and R.J.N.Phillips, Phys.Rev. 187 (1969) 2210.
- [14] G.Girardi et al., Nucl.Phys. B47 (1972) 445.
- [15] V.Garsevanishvili et al, JINR preprint (1972).
- [16] J.Deregel et al., Phys.Lett. 43B (1973) 338.

TABLE CAPTIONS.

Table 1. Definition of the polarization parameters P, R and A by the expressions relating final and initial polarization components on the laboratory system. See text for definition of  $\vec{k}_i$ ,  $\vec{k}_f$ ,  $\vec{k}_p$  and  $\hat{n}$ .

Table 2. Expressions relating observables and s-channel helicity amplitudes.

Table 3. Polarization experiments in pion-nucleon elastic scattering above 6 GeV/c incident momentum (July 1973).

FIGURE CAPTIONS.

- Fig. 1a Polarization P in  $\pi^+p$  elastic scattering [1-3]
- Fig. 1b Polarization P in  $\pi^-p$  elastic scattering [1-3]
- Fig. 2 Polarization P in  $\pi^-p$  charge exchange [4]
- Fig. 3a Spin-rotation parameter R in  $\pi^+p$  elastic scattering at 6 GeV/c [5]
- Fig. 3b Spin-rotation parameter R in  $\pi^-p$  elastic scattering at 6 GeV/c [5]
- Fig. 3c Spin-rotation parameter R in  $\pi^-p$  elastic scattering at 16 GeV/c [5]
- Fig. 4 Moduli of s-channel helicity amplitudes at 6 GeV/c [7]
- Fig. 5 Complex ratios of s-channel helicity amplitudes at 6 GeV/c [7]
- Fig. 6 Predictions for R and A in pion-nucleon charge exchange at 6 GeV/c [7]
- Fig. 7 Real and imaginary parts of the s-channel helicity non-flip amplitudes for isospin T = 1 exchange. (See text for hypothesis about the phase of  $F_{++}^{\circ}$ .)
- Fig. 8 Real and imaginary parts of the s-channel helicity flip amplitude for isospin T = 1 exchange. (See text for hypothesis about the phase of  $F_{++}^{\circ}$ .)
- Fig. 9a Schematic views of target and detectors used for simultaneous P and R measurements [10,11]
- Fig. 9b Detectors for R measurements, horizontal plane.
- Fig. 9c Detectors for P measurements, vertical plane [10]
- Fig. 10 Preliminary data for P in  $\pi^-p$  elastic scattering at 40 GeV/c [11]  
The curves show the theoretical values taken from refs. [12-15]

... / ...

- Fig. 11 Energy variation of the first minimum of the polarization  $P_0$  in  $\pi^-p$  elastic scattering averaged over a momentum transfer interval between  $t = -0.1$  and  $-0.3$   $(\text{GeV}/c)^2$ . The straight line represents a fit  $P_{\text{AVR}} = -(0.48 \pm 0.06) s^{-(0.52 \pm 0.05)}$ . [10]
- Fig. 12 Energy variation of the polarization  $P_0$  in  $\pi^-p$  elastic scattering averaged over a momentum transfer interval between  $t = -1.0$  and  $-1.4$   $(\text{GeV}/c)^2$ .
- Fig. 13 Preliminary data for  $P$  in  $K^-p$  elastic scattering at  $40$   $\text{GeV}/c$  [11]. The curve shows the theoretical values for  $P$  at  $50$   $\text{GeV}/c$  taken from ref. [14].
- Fig. 14 Energy variation of the polarization  $P_0$  in  $K^-p$  elastic scattering at  $t \simeq -0.6$   $(\text{GeV}/c)^2$ .
- Fig. 15 Preliminary data for  $R$  in  $\pi^-p$  elastic scattering at  $40$   $\text{GeV}/c$ . The curves show the predictions by the models [13] and [14] respectively.
- Fig. 16 Spin-rotation parameter  $C = 0.999 R + 0.052 A$  in proton-proton elastic scattering at  $6.0$  and  $15.75$   $\text{GeV}/c$  [16]. The solid line represents the function  $-\cos \Theta_p$  (see text).



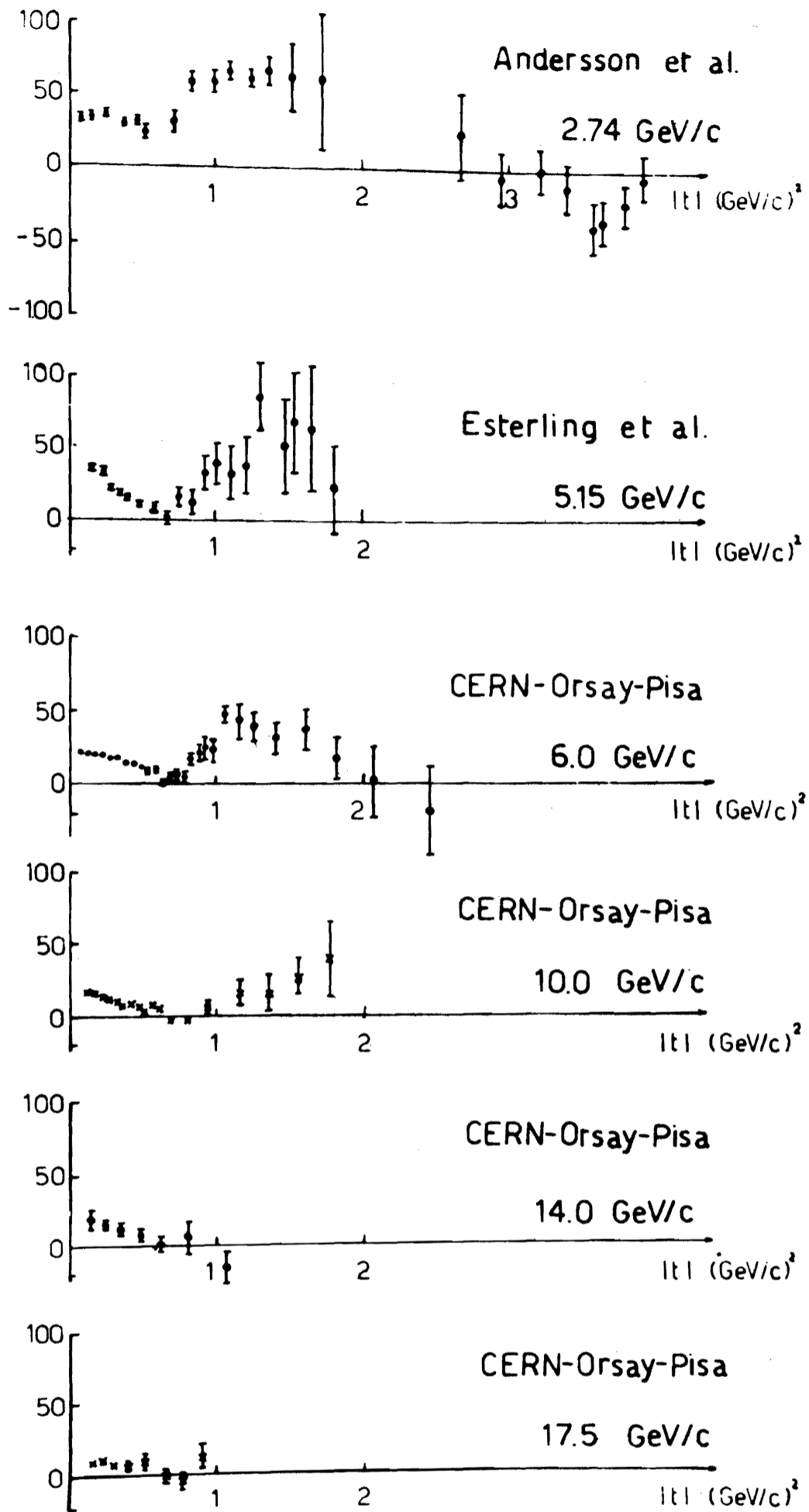


FIG. 1A

$\pi^+$  p polarization results  
- 220 -

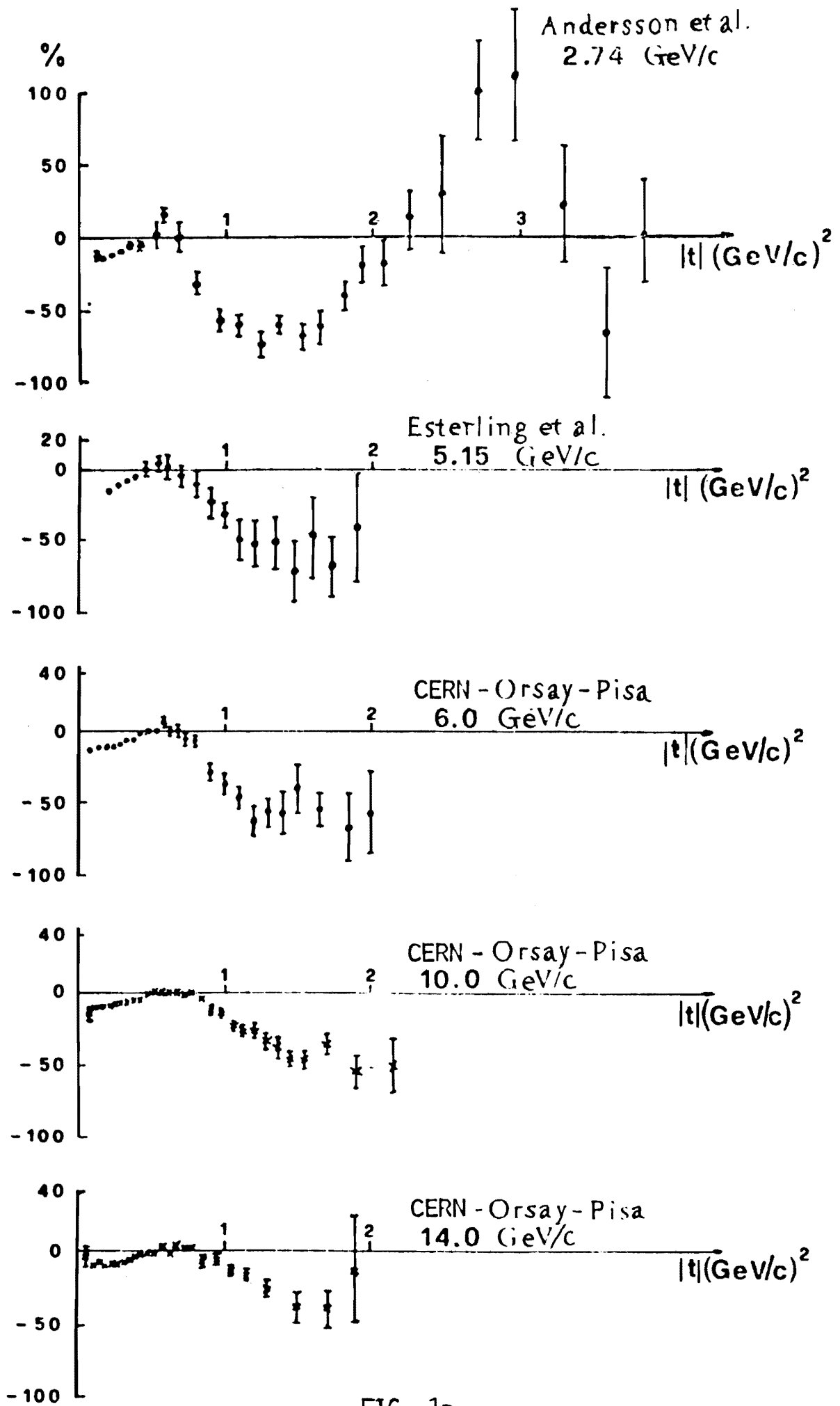


FIG. 1B

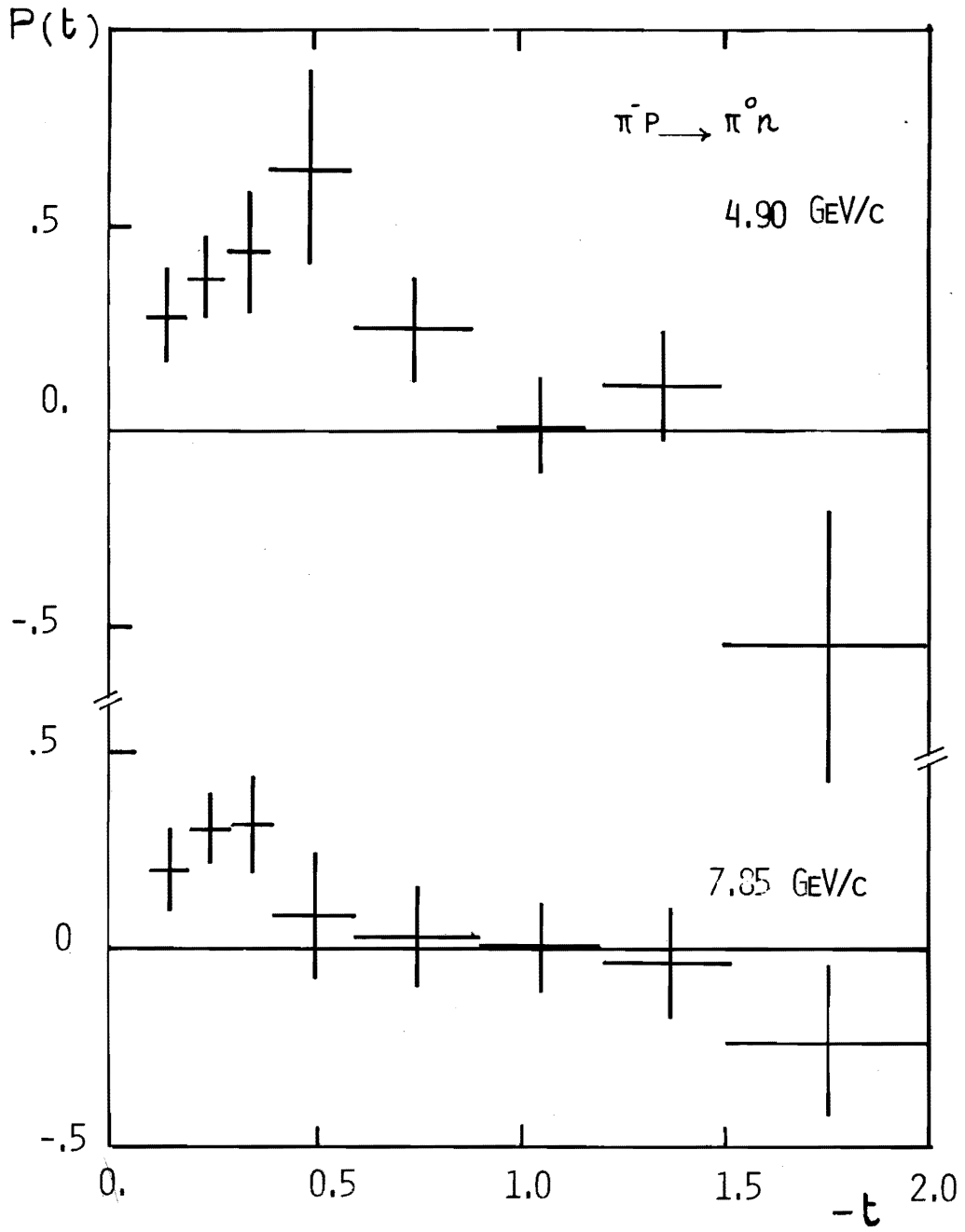


FIG.2

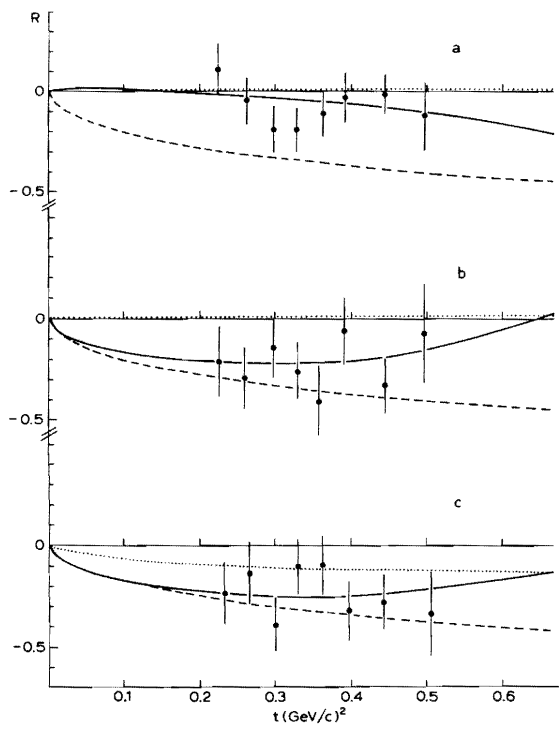


FIG. 3

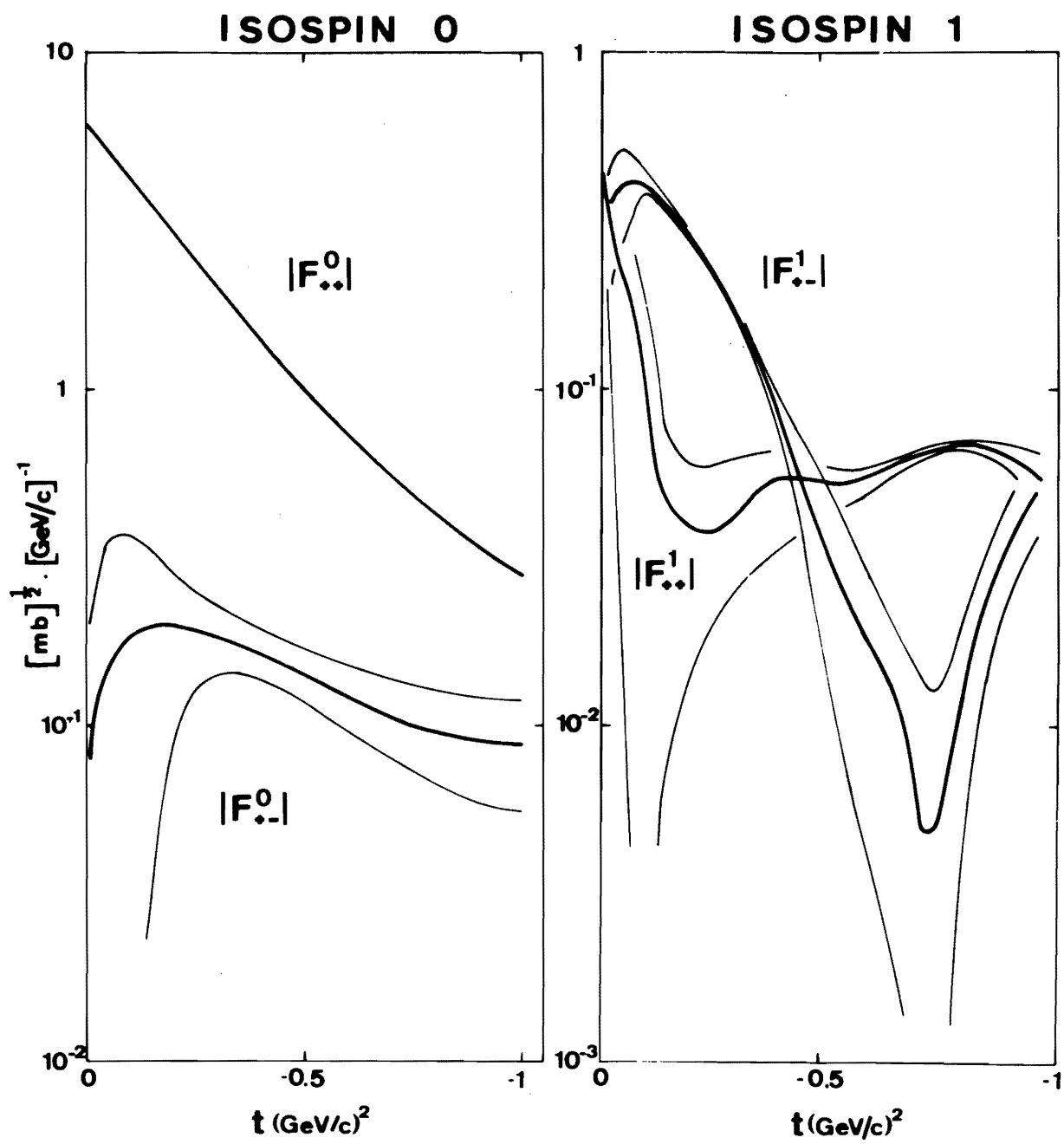


FIG. 4

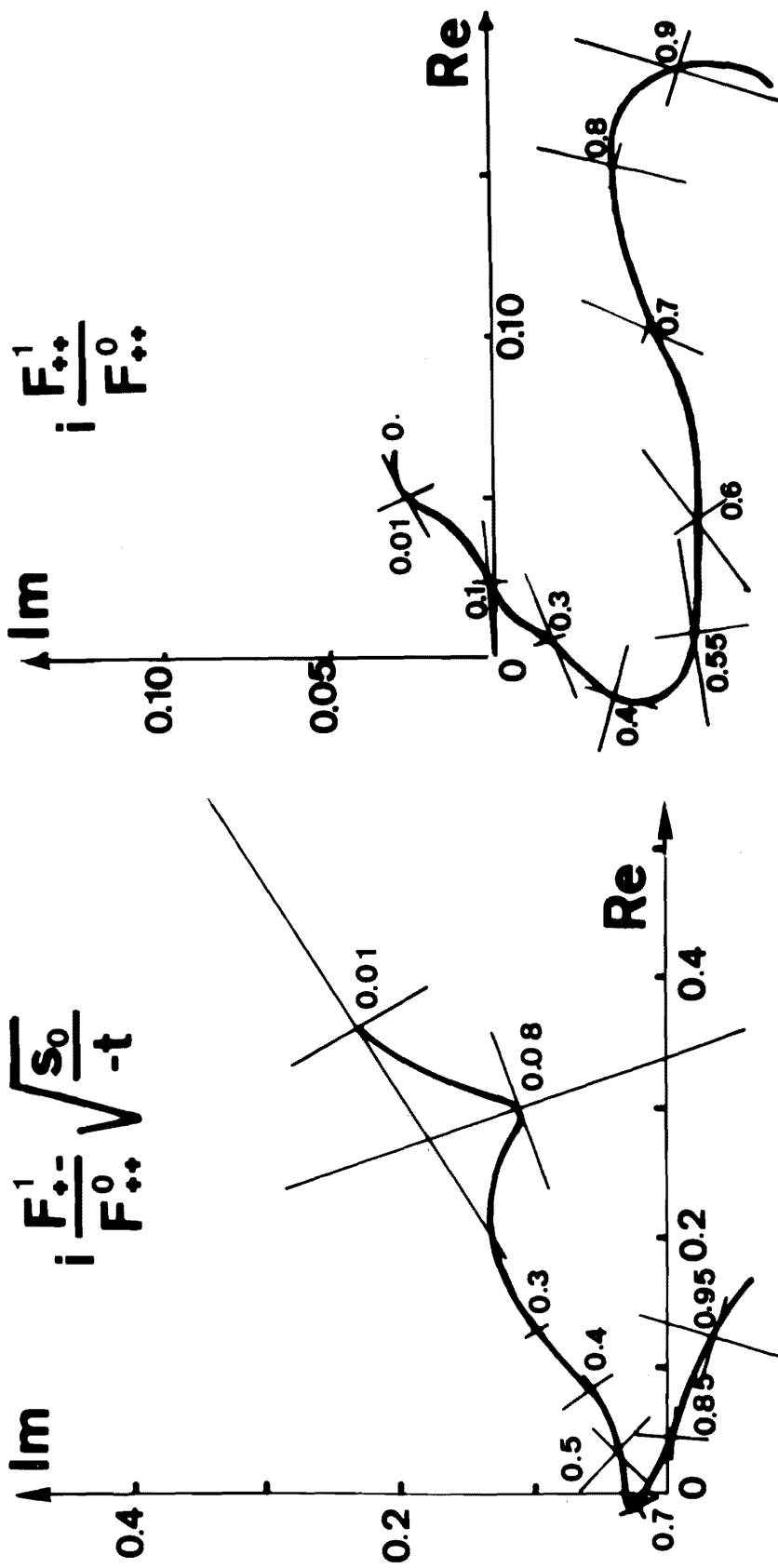


FIG. 5

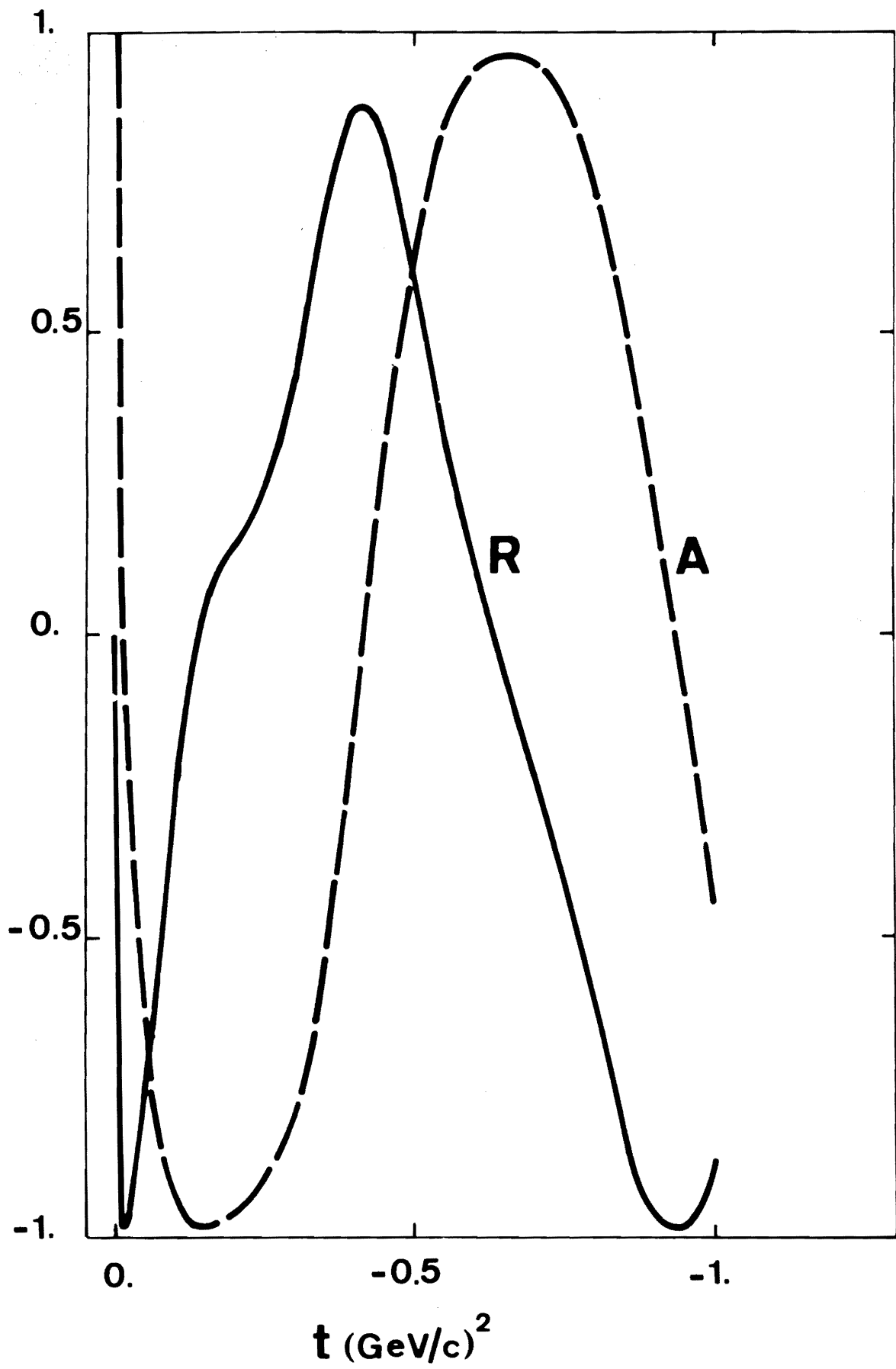
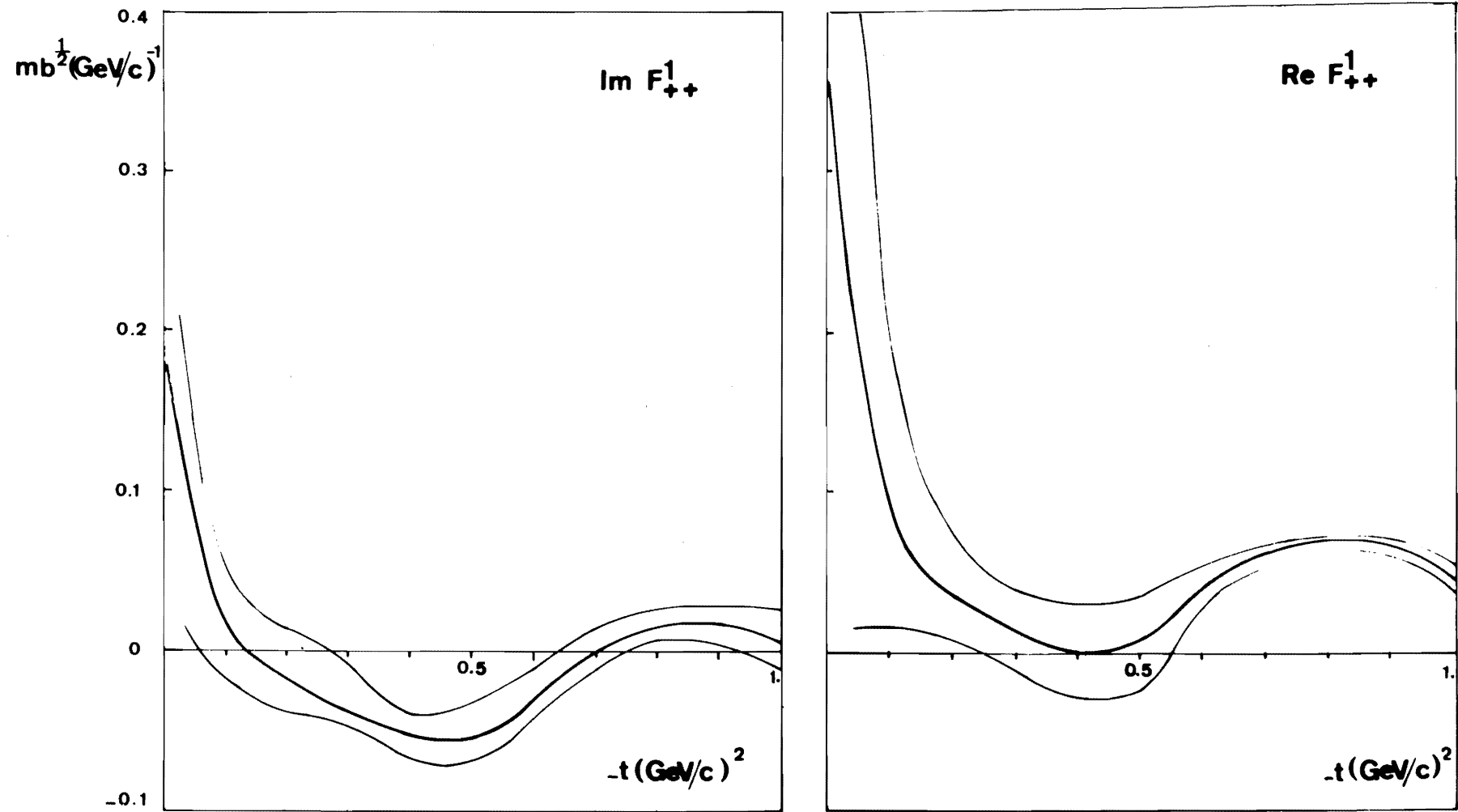


FIG. 6

π N ISOPIN T=1 EXCHANGE  
HELICITY NON-FLIP

6 GeV/c



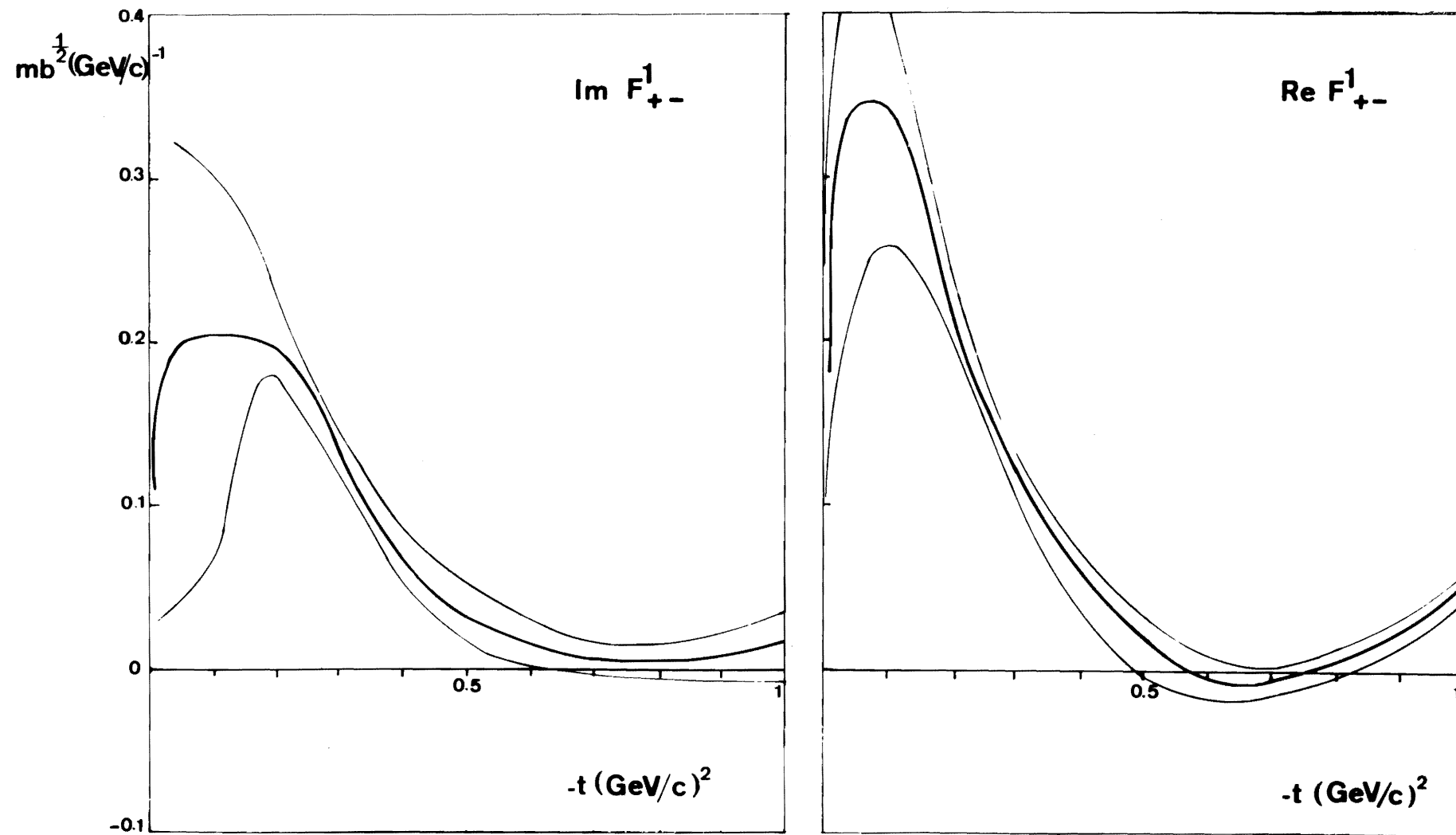
- 227 -

FIG. 7



πN ISOSPIN T=1 EXCHANGE  
HELICITY FLIP

6 GeV/c



- 228 -

FIG. 8

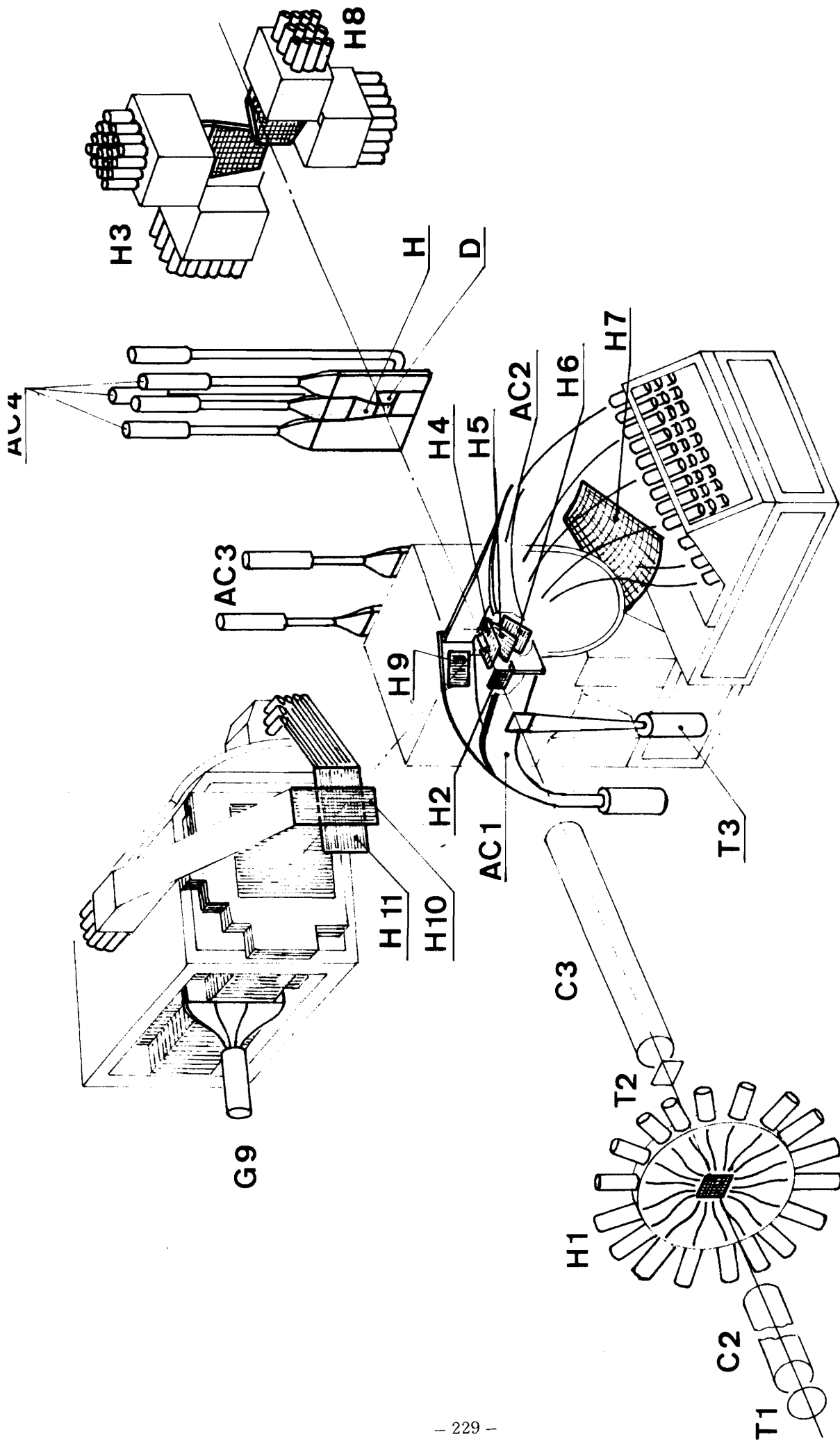
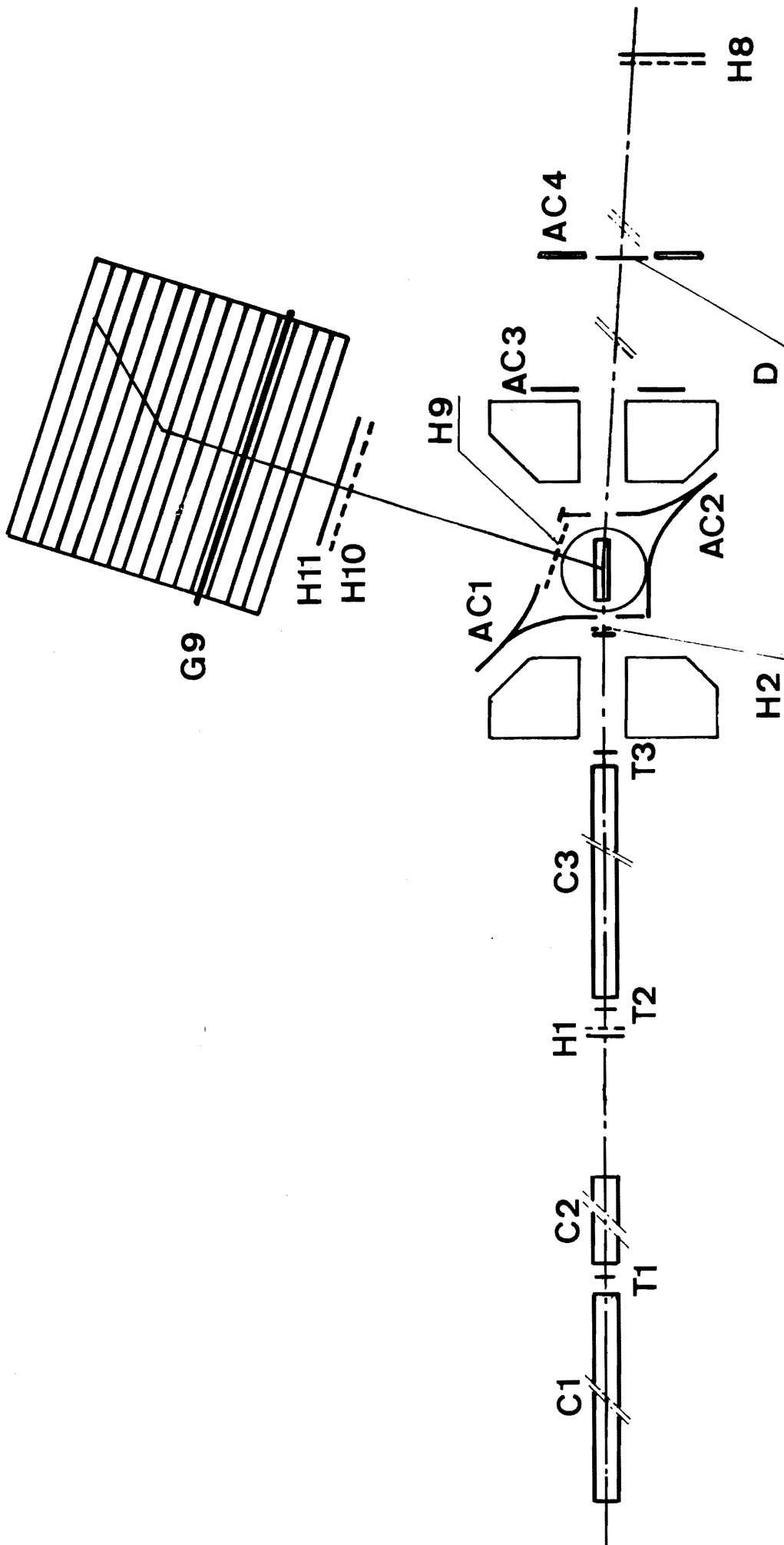


FIG. 9A



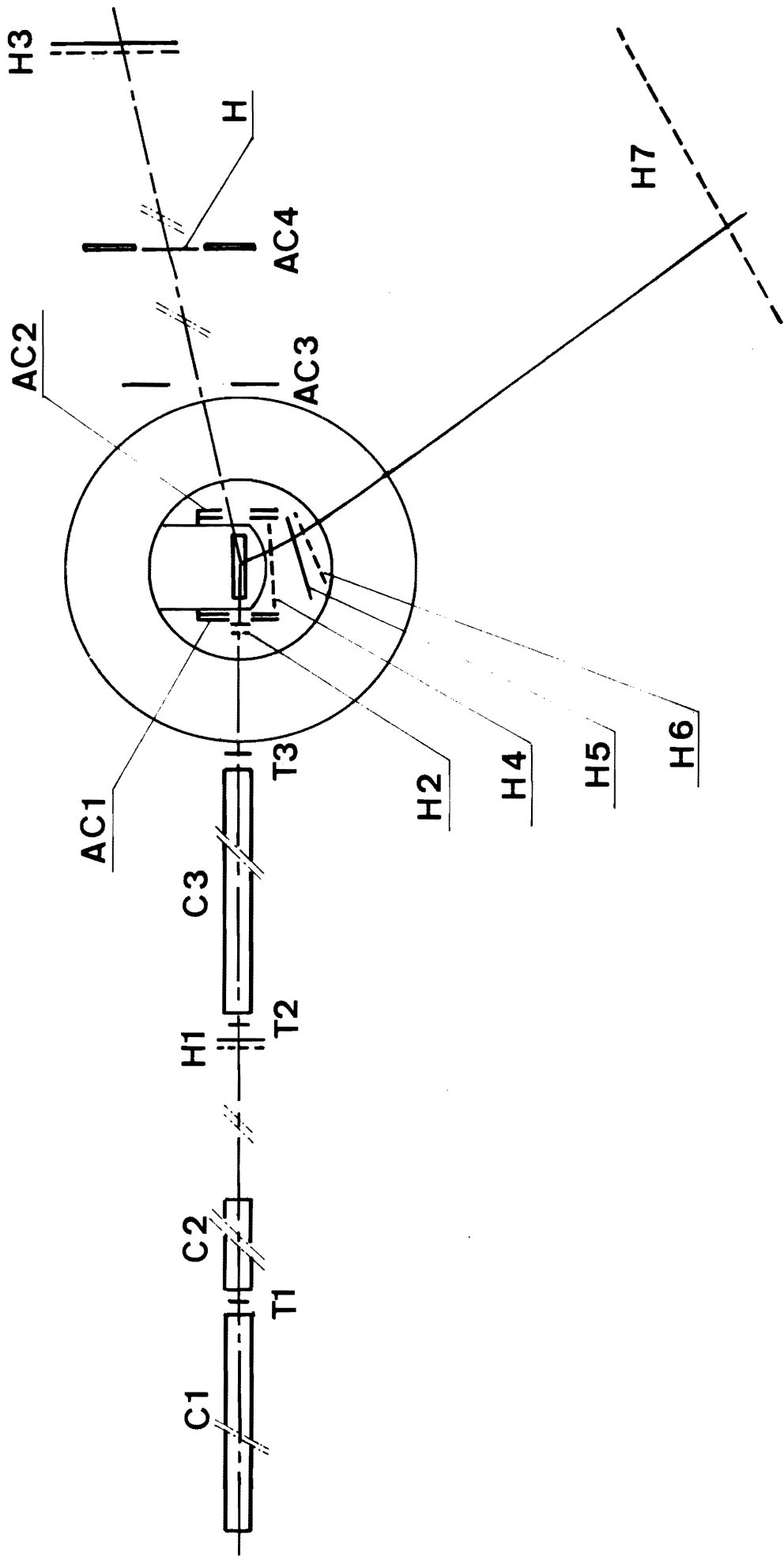


FIG. 9c

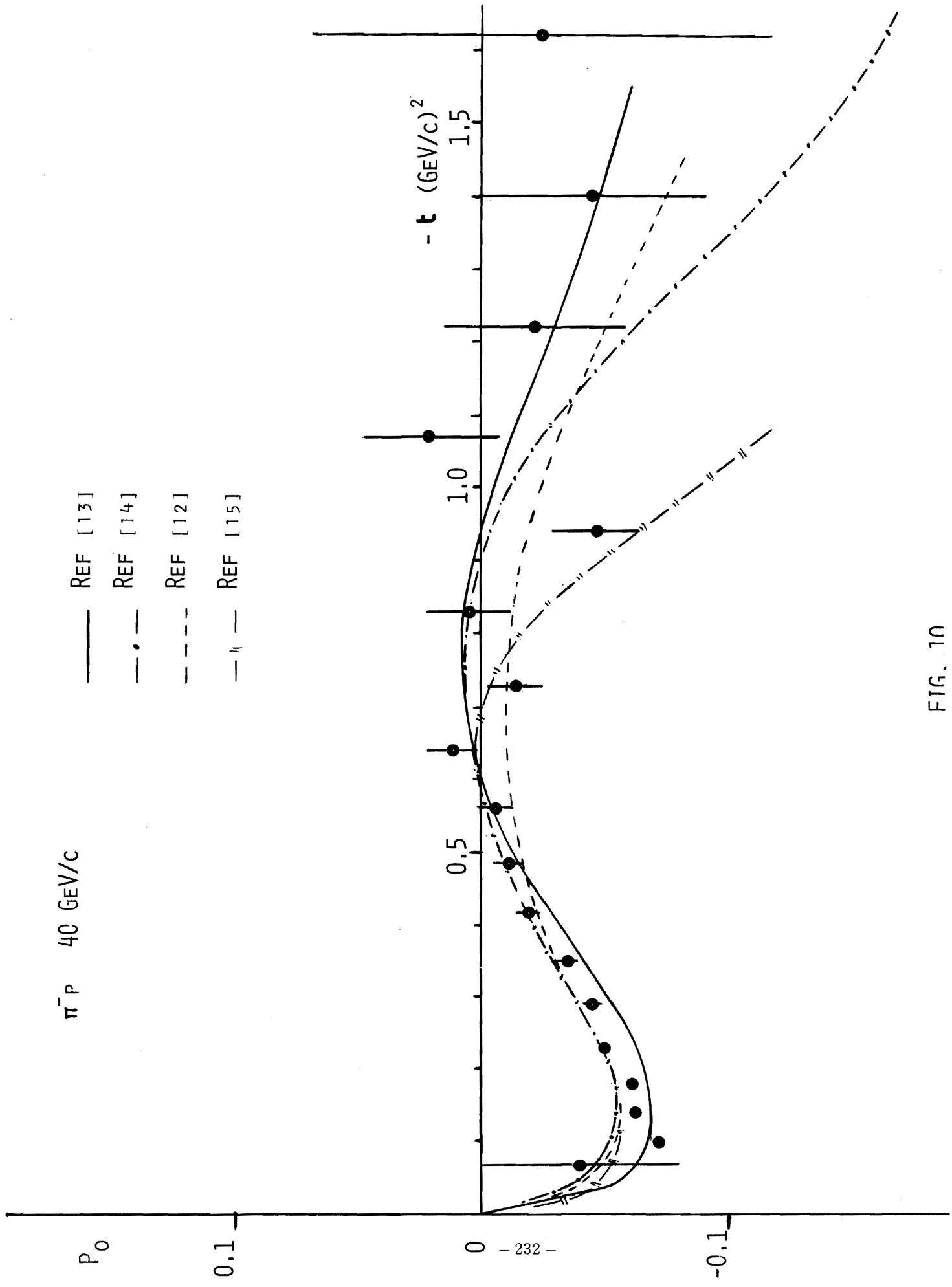


FIG. 10

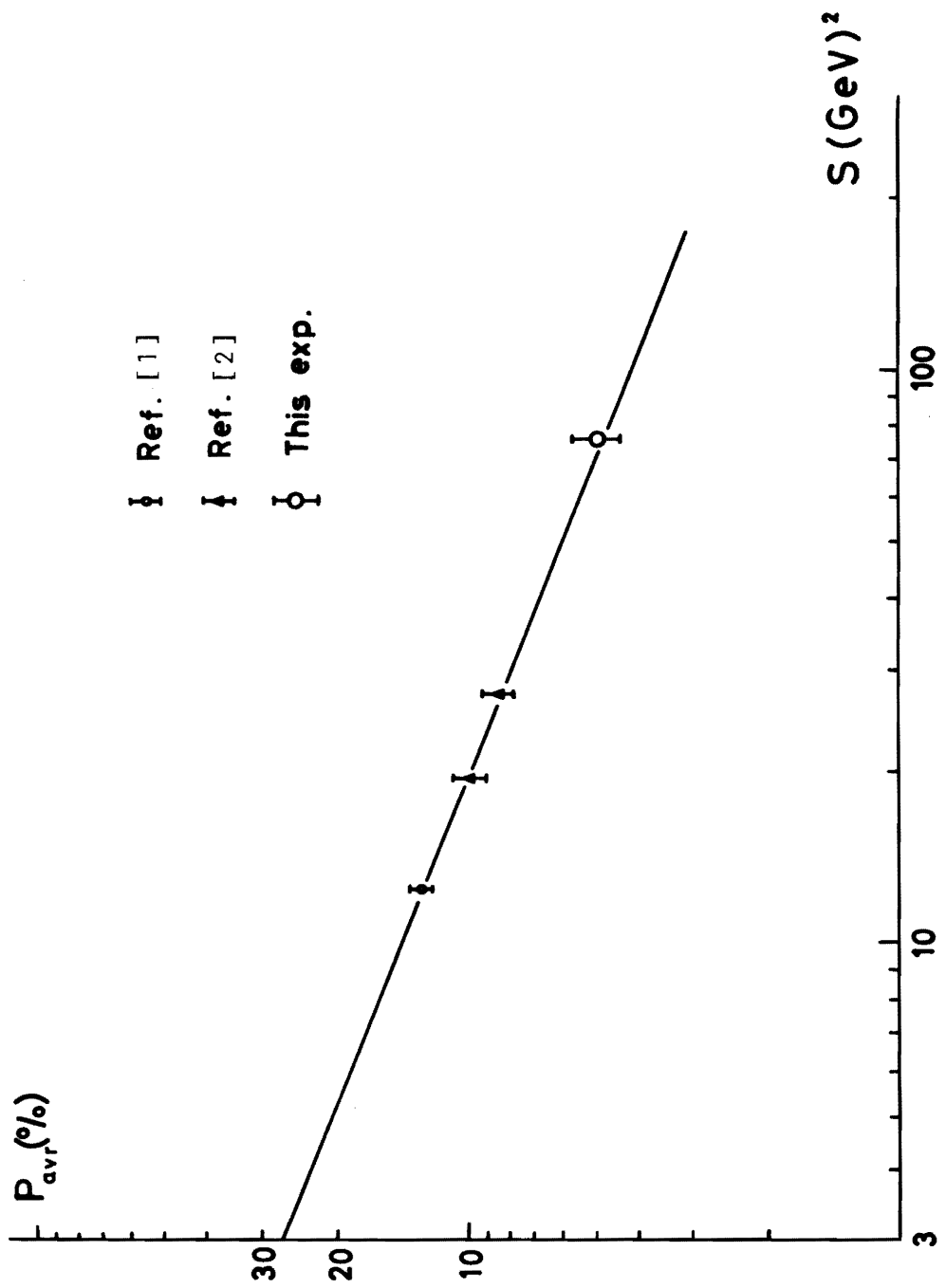


FIG. 11

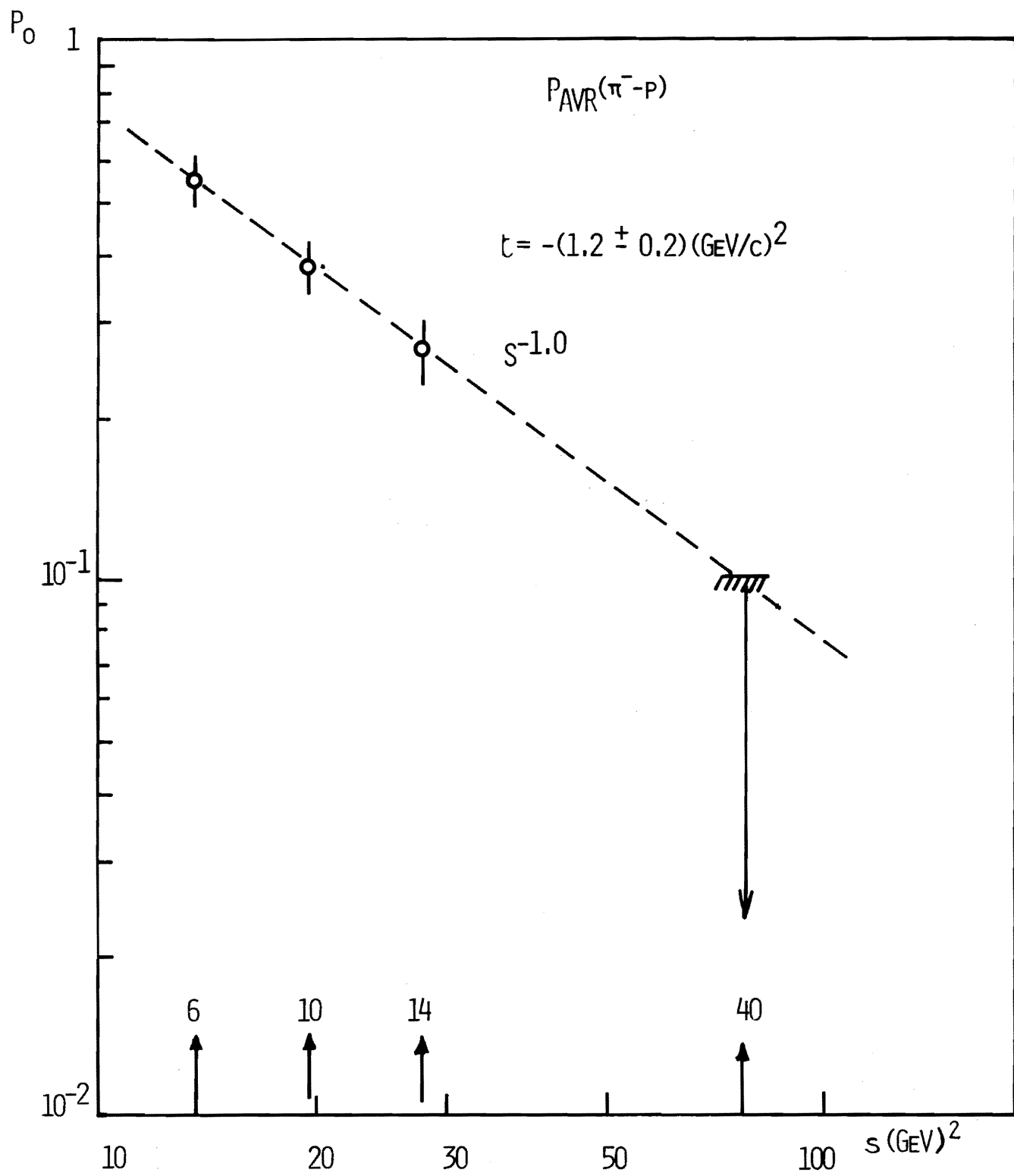


FIG. 12

$K^-P$  40 GEV/C

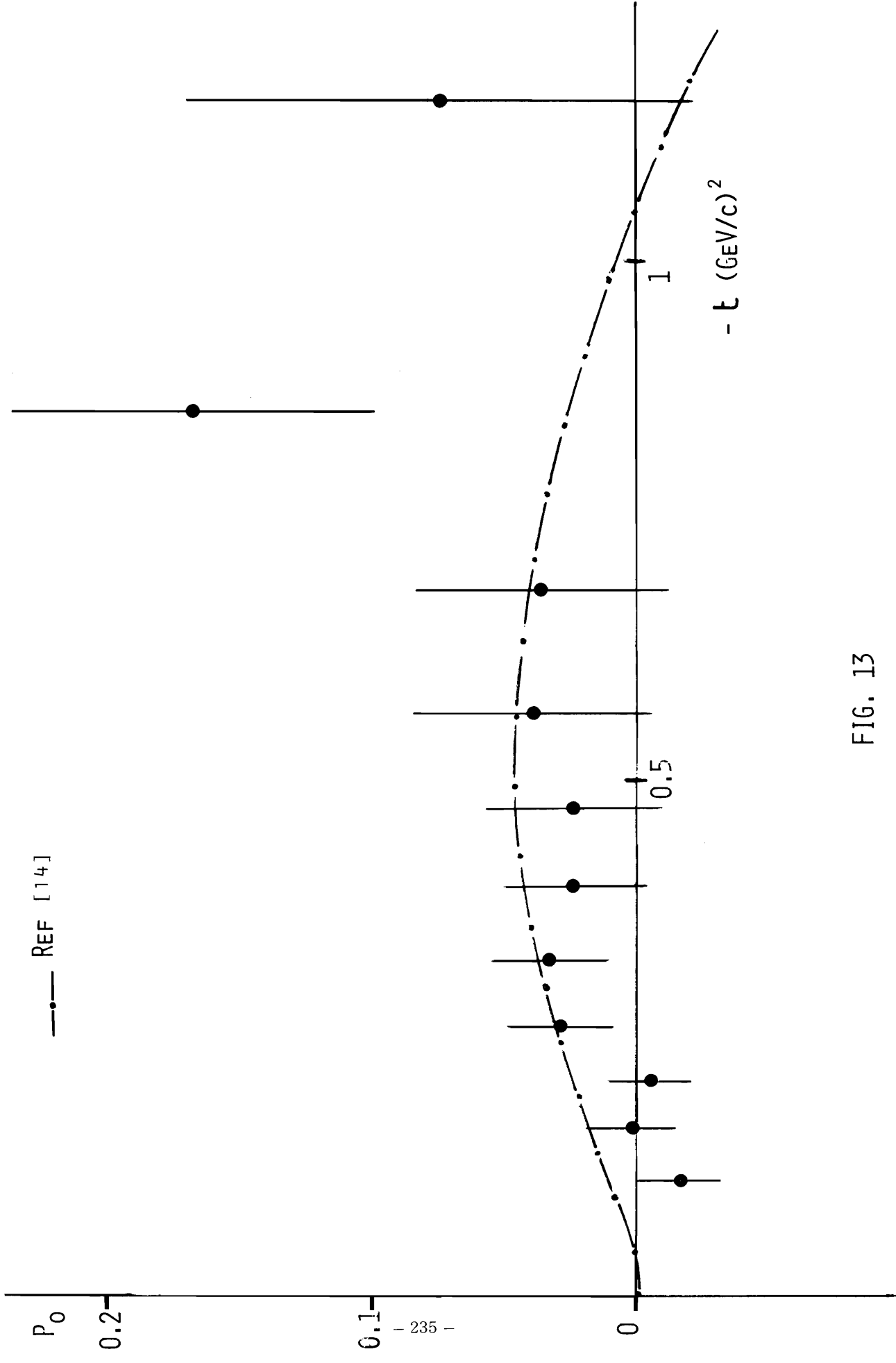


FIG. 13



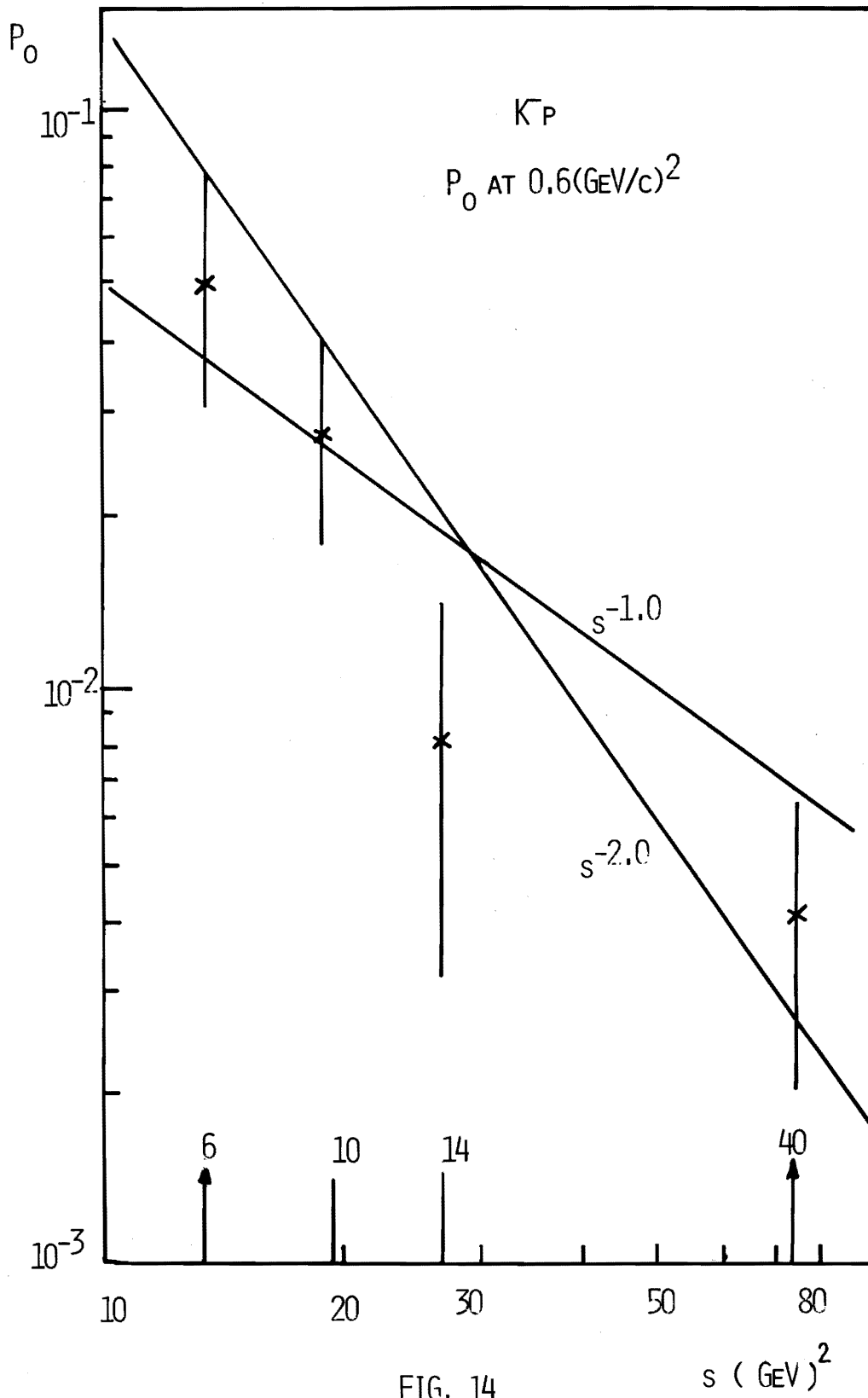


FIG. 14

R  $\pi^-p$  40 GeV/c

- BARGER & PHILLIPS [13]
- - - GIRARDI ET AL. [14]
- - -  $-\cos\theta_p$

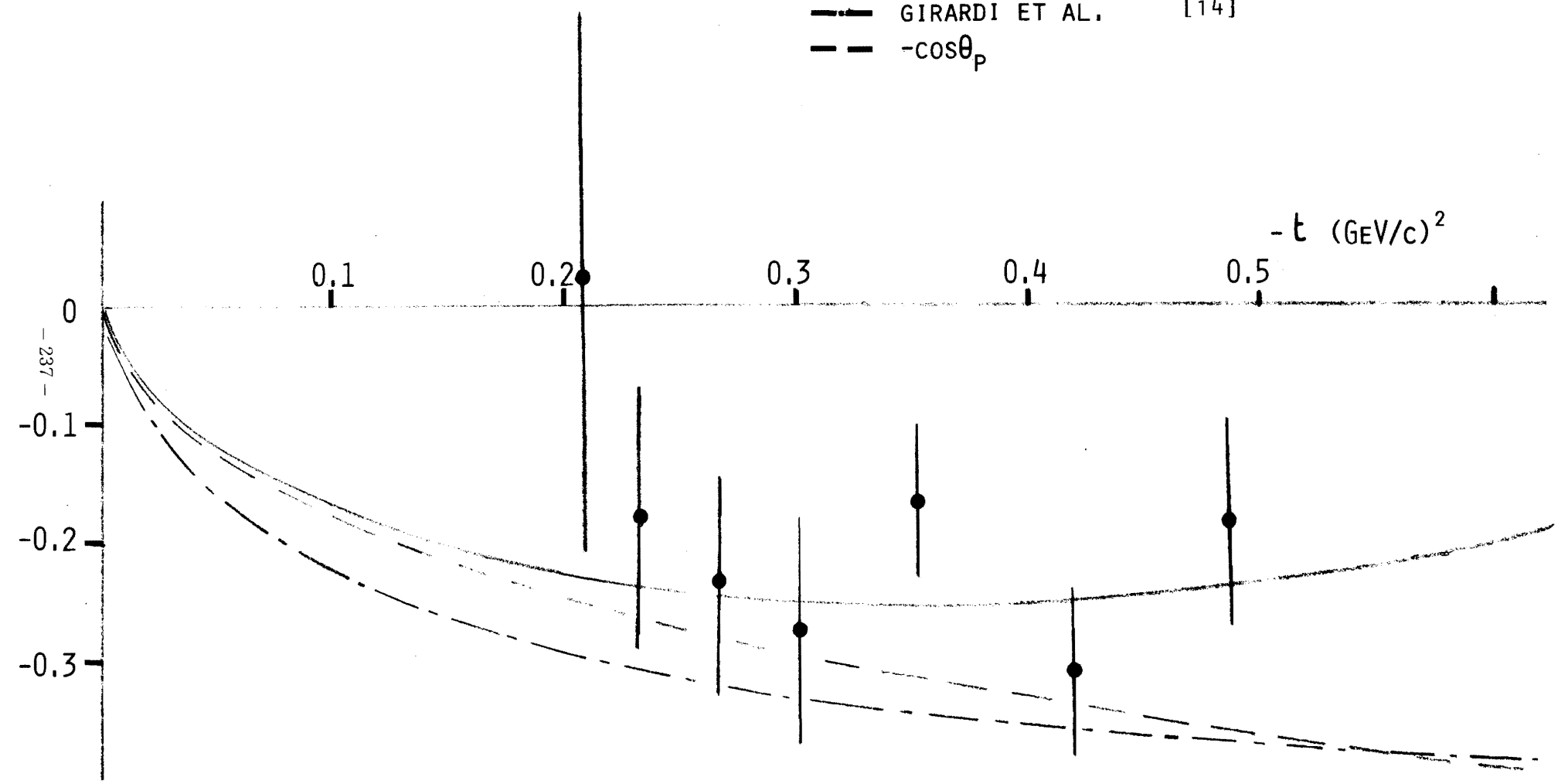


FIG. 15

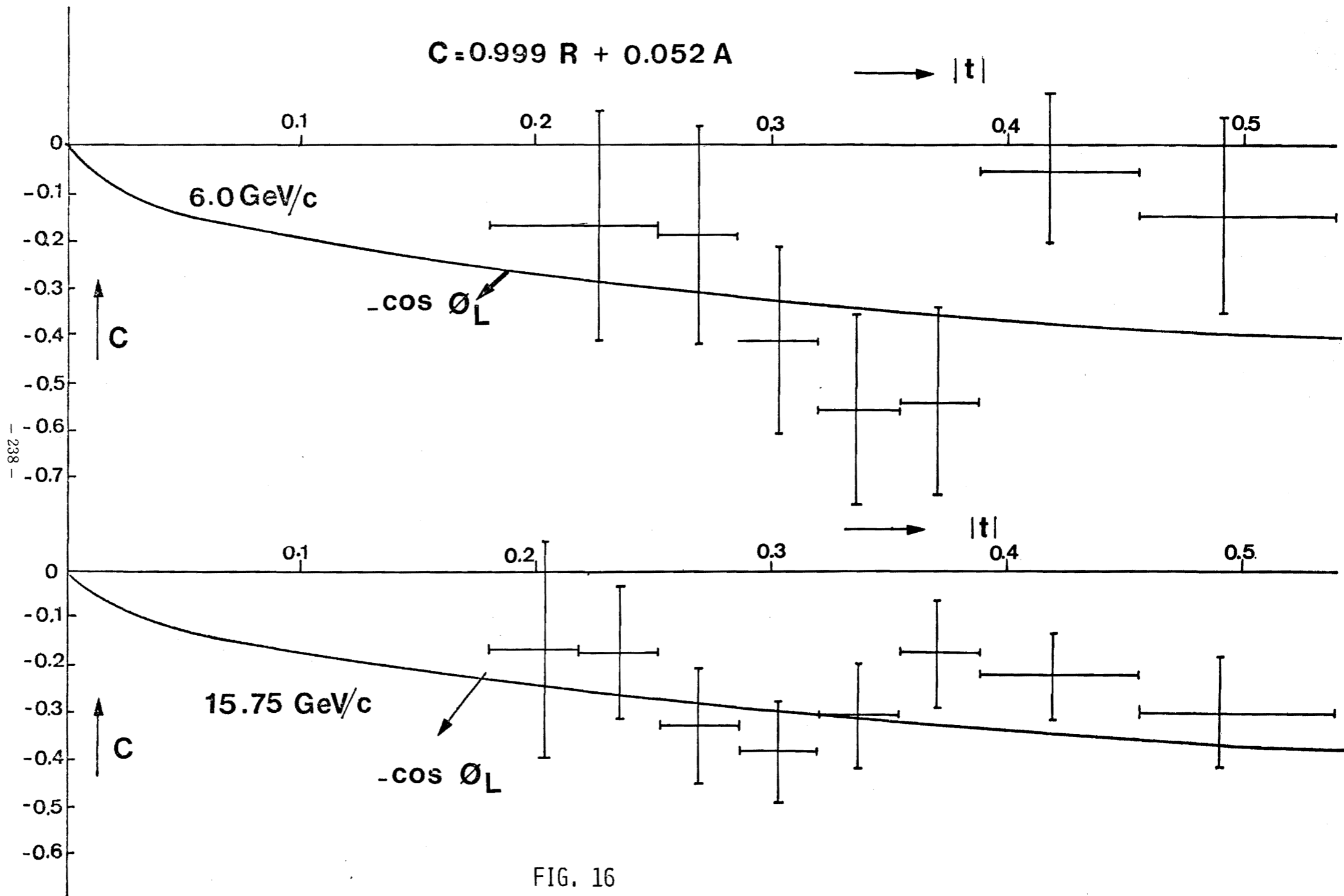


FIG. 16